

Electrodisintegration of ^{63}Cu and ^{65}Cu

M. N. Martins, E. Wolyneć, and M. C. A. Campos

Instituto de Física da Universidade de São Paulo, São Paulo, S.P., Brazil

(Received 2 August 1982)

The (e,α) cross section for ^{65}Cu has been measured in the electron energy range 14–34 MeV. The results have been analyzed using the distorted-wave Born approximation $E1$ and $E2$ virtual photon spectra and the $E1$ and $E2$ components of the corresponding (γ,α) cross section were obtained. To assess the accuracy of the virtual photon analysis, the $(e,2n)$ cross section for ^{63}Cu was also measured and the obtained $(\gamma,2n)$ cross section is compared with direct measurement of this cross section performed with annihilation gamma rays.

$$\left[\begin{array}{l} \text{NUCLEAR REACTIONS } ^{65}\text{Cu}(e,\alpha) \text{ and } ^{63}\text{Cu}(e,2n). \text{ Measured} \\ \sigma_{e,\alpha}(E_0) \text{ and } \sigma_{e,2n}(E_0). \text{ Deduced } \sigma_{\gamma,\alpha}^{E1}(E), \sigma_{\gamma,\alpha}^{E2}(E), \text{ and } \sigma_{\gamma,2n}^{E1}(E). \end{array} \right]$$

I. INTRODUCTION

The (e,α) cross section has been measured for several nuclei^{1,2} and the results have been analyzed using DWBA virtual photon spectra^{3,4} to obtain the $E1$ and $E2$ components of the corresponding (γ,α) cross section.

In this paper we use the same technique described in Refs. 1 and 2 to study the (e,α) cross section in ^{65}Cu . This technique takes advantage of the fact that the $E2$ virtual photon spectrum is enhanced relative to the $E1$ spectrum, as shown in Fig. 1, while the bremsstrahlung spectrum contains all multipoles in equal amounts. The $E1$ and $E2$ components of the (γ,α) cross section are obtained from combined measurements of the electrodisintegration cross section and the corresponding yield of electrodisintegration plus photodisintegration in-

duced by bremsstrahlung.

The (γ,α) cross section is known for many nuclei and in almost all studied cases it has a resonant shape. However, for two nuclei, ^{90}Zr (Ref. 5) and ^{65}Cu (Ref. 6), the (γ,α) cross section, obtained from measurements of the (e,α) cross section, showed a nonresonant behavior. For these nuclei the (γ,α) cross section increases continuously with the photon energy up to the maximum energy studied, which was ~ 60 MeV. An attempt was made to explain the strange behavior of the (γ,α) cross section in ^{90}Zr , using a preequilibrium exciton model combined with the quasideuteron model.⁵

This has motivated us to study the (e,α) cross section in ^{65}Cu , since it can easily be measured by residual activity. In Ref. 6 the (e,α) cross section was measured by directly counting the alpha particles emitted at 90° to the electron beam.

In order to assess the accuracy of the technique employed in the analysis we have measured the $(e,2n)$ cross section for ^{63}Cu . There are several reasons for this choice. The $(\gamma,2n)$ cross section is well known for this nucleus and it is above the isoscalar $E2$ and below the isovector $E2$ resonances. Thus we can be sure it is an $E1$ process. Even though there are many experimental tests of the $E1$ virtual photon spectra, and all show excellent agreement between calculation and experiment, it has been pointed out by Ströher⁷ that no conclusive tests of the $E1$ virtual photon spectra exist, since the investigated reaction data were analyzed with the assumption of a pure $E1$ excitation, in cases where $E2$ excitation could give a significant contribution. Furthermore, the $(e,2n)$ cross section can

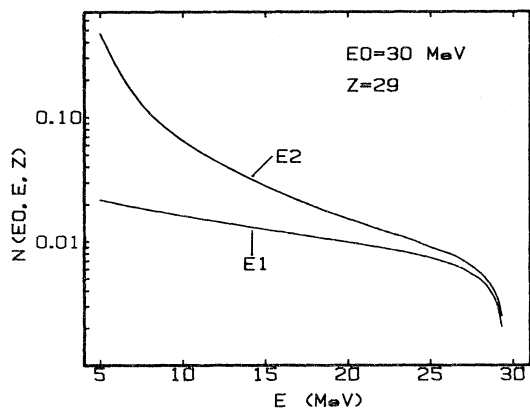


FIG. 1. $E1$ and $E2$ virtual photon spectra for 30 MeV electrons inelastically scattered from a copper nucleus.

TABLE I. Target properties and separation energies.

Target	^{63}Cu	^{65}Cu
Enrichment (%)	99.89	99.69
Thickness (mg/cm ²)	10.06±0.10	9.86±0.10
$S(2n)$, MeV	19.7	17.8
$S(\alpha)$, MeV	5.8	6.76

also be measured by radioactivity and yields the same gamma ray line used to measure the (e,α) cross section, as discussed in the next section. Consequently, the results also test the reliability of our measurements.

II. THE EXPERIMENT

The experiment was performed using the electron linear accelerator of Universidade de São Paulo. Table I gives target thicknesses and enrichments. The (e,α) and $(e,2n)$ cross sections were measured by counting the induced residual activity. For the (e,α) cross section in ^{65}Cu we measured the 67.4 keV gamma ray which follows the decay of $^{61}\text{Co} \rightarrow ^{61}\text{Ni} + \beta^-$, with a half-life of (1.650 ± 0.005) h.⁸ For the $(e,2n)$ cross section we measured the same 67.4 keV gamma ray, since ^{61}Cu decays to ^{61}Ni with a half-life of (3.41 ± 0.01) h.⁹ Figure 2 shows a typical gamma ray spectrum. It is important to notice that there are no nearby lines which could contribute to uncertainties in deriving the cross sections. As a check of our data, we measured both half-lives after irradiating the targets with 30 MeV electrons, and the decay constants obtained are compared with values from the literature in Table II.

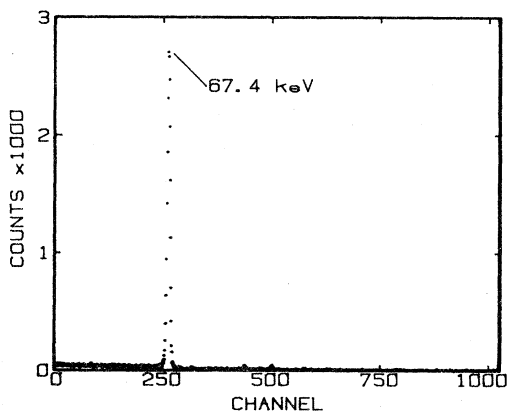


FIG. 2. Typical gamma ray spectrum observed in the decay of ^{61}Co , obtained from the reaction $^{65}\text{Cu}(e,\alpha)^{61}\text{Co}$.

TABLE II. Decay constants.

Nucleus	λ (min ⁻¹)	Ref.
^{61}Co	$(6.95 \pm 0.29) \times 10^{-3}$	This work
	$(7.001 \pm 0.021) \times 10^{-3}$	8
^{61}Cu	$(3.56 \pm 0.18) \times 10^{-3}$	This work
	$(3.39 \pm 0.01) \times 10^{-3}$	9

In order to obtain the electrodisintegration plus photodisintegration yields, a 0.717 g/cm² copper radiator was placed in the electron beam, ahead of the target, without any spacing between the radiator and the target.

III. RESULTS AND ANALYSIS

The electrodisintegration cross section $\sigma_{e,x}(E_0)$ may be obtained from the photonuclear cross section $\sigma_{\gamma,x}^{\lambda L}(E)$ through an integral over the virtual photon spectrum $N^{\lambda L}(E_0, E, Z)$:

$$\sigma_{e,x}(E_0) = \int_0^{E_0 - m} \sum_{\lambda L} \sigma_{\gamma,x}^{\lambda L}(E) \times N^{\lambda L}(E_0, E, Z) \frac{dE}{E}. \quad (1)$$

In Eq. (1), E_0 stands for the total electron energy and E stands for the excitation energy of multipolarity λL . In the same spirit the yield with the radiator in is

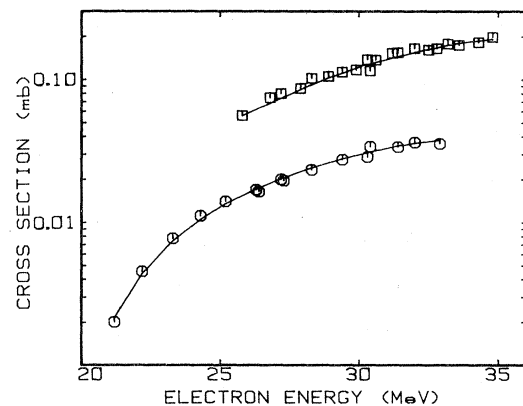


FIG. 3. $\sigma_{e,2n}(E_0)$ for ^{63}Cu (circles) and the yield of electrodisintegration plus photodisintegration (squares). The smooth curves are the best fit to the data and were obtained by combining the histogram shown in Fig. 5 with the $E1$ virtual photon spectrum and the Davies-Bethe-Maximom (DBM) bremsstrahlung cross section in Eqs. (1) and (2).

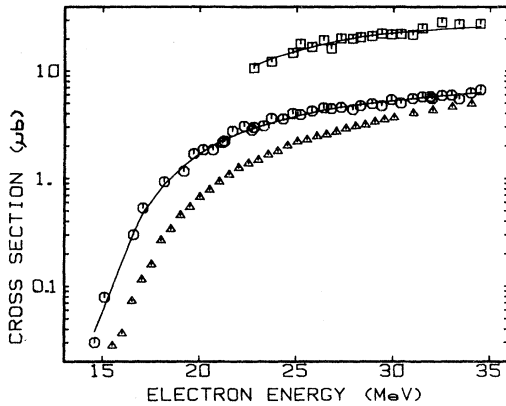


FIG. 4. $\sigma_{e,\alpha}(E_0)$ for ^{65}Cu (circles) and the yield of electrodisintegration plus photodisintegration (squares). The smooth curves are the best fit to the data and were obtained by combining the $E1$ and $E2$ histograms of Fig. 7 with the virtual photon spectra and the DBM bremsstrahlung cross section in Eqs. (1) and (2). The triangles show the (e,α) cross section from Ref. 6.

$$Y_{e,x}(E_0) = \sigma_{e,x}(E_0 - 2\Delta E_0) + N_r \int_0^{E_0 - m} \sum_{\lambda L} \sigma_{\gamma,x}^{\lambda L}(E) \times K(E_0 - \Delta E_0, E, Z_r) \frac{dE}{E}, \quad (2)$$

where N_r is the number of nuclei/cm² in the copper radiator, $K(E_0, E, Z_r)$ is the bremsstrahlung cross section in copper, and ΔE_0 is the electron energy loss in half the radiator thickness. We have used the Davies-Bethe-Maximon¹⁰ bremsstrahlung cross section. The size correction discussed in Ref. 2 was

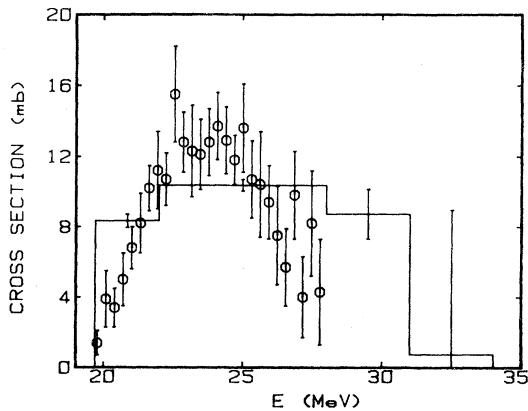


FIG. 5. $^{63}\text{Cu}(\gamma, 2n)$ cross section. The histogram is the result derived from this work and the points show the measurement of Fultz *et al.*¹

applied to the virtual photon spectra. This correction, for 35 MeV electrons, amounts to 2% for the $E1$ and 8% for the $E2$ spectra.

The measured $(e, 2n)$ and (e, α) cross sections (circles) and the corresponding yields of electrodisintegration plus photodisintegration (squares) are shown in Figs. 3 and 4. In Fig. 4 the triangles show the (e, α) cross section from Ref. 6. In order to compare it with our results, we have multiplied their 90° cross section by 4π , since previous measurements have shown that the angular distribution is nearly isotropic.^{11,12}

The cross sections $\sigma_{e,x}(E_0)$ and the yields $Y_{e,x}(E_0)$ have been simultaneously fitted, using Eqs. (1) and (2), with the photonuclear cross sections represented by histograms.

As discussed previously, for the $(\gamma, 2n)$ cross section we used only $E1$ multipolarity. The histogram in Fig. 5 shows the $(\gamma, 2n)$ cross section obtained from our measurements. The experimental points show the $(\gamma, 2n)$ cross section measured by Fultz *et al.*¹³ There is good agreement between the $(\gamma, 2n)$ cross section derived from our electrodisintegration measurement and the cross section measured with annihilation gamma rays. Our integrated $(\gamma, 2n)$ cross section, up to 27.8 MeV (the maximum energy measured by Ref. 13) is 79.3 ± 2.2 MeV mb, while Fultz obtains 76 MeV mb. The difference of 4.5% in the integrated strength is well within the uncertainties of the absolute values of both experiments.

Figure 6 shows the ratio of measured to calculated $(e, 2n)$ cross sections (circles) and measured to calculated electrodisintegration plus photodisintegration yields (triangles). This is the ratio between the measured points and the calculated full

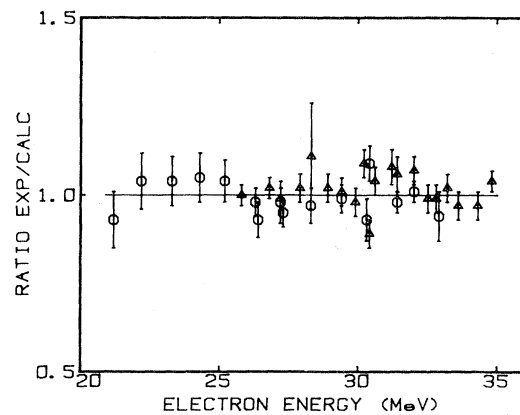


FIG. 6. Ratio of measured to calculated $(e, 2n)$ cross section (circles) and measured to calculated yield of electrodisintegration plus photodisintegration (triangles).

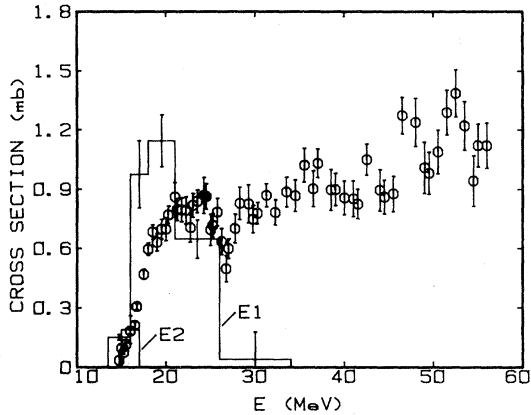


FIG. 7. $^{65}\text{Cu}(\gamma, \alpha)$ cross sections. The $E1$ and $E2$ histograms are the results from this work. The points show the (γ, α) cross section from Ref. 6.

curves of Fig. 3. This figure shows the compatibility between electrodisintegration and photodisintegration, that is, between the $E1$ virtual photon spectrum and the bremsstrahlung spectrum. These results give confidence to our measurement and the analysis employed to derive the photonuclear cross section.

Figure 7 shows the histograms obtained for the $E1$ and $E2$ components of the (γ, α) cross section. The $E1$ component exhausts 0.97 ± 0.14 percent of the dipole sum and the $E2$ component 3.2 ± 1.2 percent of the energy weighted sum rule for isoscalar $E2$. The points show the (γ, α) cross section from Ref. 6, multiplied by 4π . It was obtained by the unfolding of the (e, α) cross section assuming a pure $E1$ process, but this would introduce only a small error in the derived (γ, α) cross section. The strong

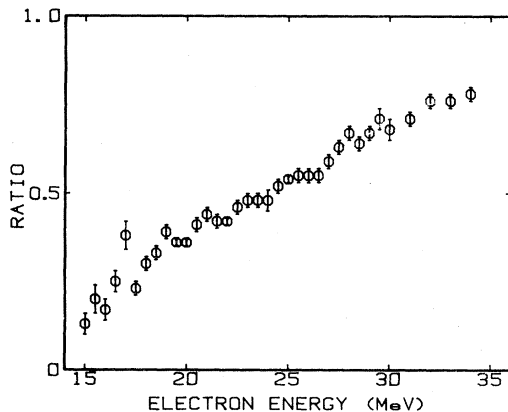


FIG. 8. Ratio of the (e, α) cross section from Ref. 6 and this work.

TABLE III. (γ, α) strength for nuclei in the $A = 60$ region. $E1$ sum: $60 NZ/A$ MeV mb; $E2$ sum: $0.22Z^2 A^{-1/3}$ $\mu\text{b}/\text{MeV}$.

Nucleus	$\int_0^{30} \sigma_{\gamma, \alpha}(E) dE$ (MeV mb)	Fraction of $E1$ sum	Fraction of $E2$ sum	Ref.
^{56}Fe	21 ± 3	2.1 ± 0.3	7 ± 1	2
^{58}Ni	43 ± 4	3.9 ± 0.4	21 ± 3	1
^{59}Co	17 ± 2	1.7 ± 0.2	5 ± 1	2
^{60}Ni	41 ± 4	3.5 ± 0.4	21 ± 5	1
^{62}Ni	17 ± 2	1.5 ± 0.2	8 ± 2	1
^{64}Zn	78 ± 16	6.9 ± 1.5	25 ± 3	2
^{65}Cu	10 ± 1	1.0 ± 0.1	3 ± 1	This work

disagreement between our (γ, α) cross section and that from Ref. 6 does not come from the analysis, but from disagreement in the experimental data. In Fig. 8 we show the ratio between the (e, α) cross section of Ref. 6 and the present measurement. Their cross section is only 0.13 of our value at 15 MeV and reaches 0.79 of our value at 34 MeV.

In Table III we compare the $E1$ and $E2$ strengths in the (γ, α) cross section of ^{65}Cu with other nuclei in this mass region. The (γ, α) cross section in ^{65}Cu is smaller than for other nuclei, but like the other nuclei studied, the $E2$ component exhausts a larger fraction of the $E2$ sum, relative to the $E1$. The strength of the (γ, α) cross section shows large variations in these nuclei, being 78 MeV mb for ^{64}Zn and only 10 MeV mb for ^{65}Cu . However, these large differences result mostly from differences in binding energies, Coulomb barrier heights, and competition with other channels, as already pointed out by Dodge *et al.*² The (γ, α) cross section in ^{65}Cu is similar in shape and magnitude to ^{62}Ni or ^{59}Co . The dominant statistical nature of the (γ, α) cross section in the nuclei listed in Table III is evident from the spectrum of the emitted alpha particles, which is of evaporation type, peaking at the energy of the Coulomb barrier.^{1,2} In the present work we did not observe the emitted alpha particles, but their spectrum is known from previous work.^{11,12} It has to be pointed out that in this respect the alpha particle spectrum from ^{90}Zr (Ref. 5) is also of the evaporation type, peaking at the energy of the Coulomb barrier height. Since, now, the only nucleus with a nonresonant (γ, α) cross section is ^{90}Zr , the results obtained for ^{65}Cu suggest that the ^{90}Zr (e, α) cross section should be measured again before developing calculations for reaction mechanisms involving cascade processes that could account for a nonresonant (γ, α) cross section.⁵

IV. CONCLUSIONS

The measurement of the $(e,2n)$ and $(e+\gamma,2n)$ cross sections for ^{63}Cu tests the $E1$ virtual photon spectrum in a situation where $E2$ contributions can be ruled out. The agreement between photodisintegration and electrodisintegration is very good. The $(\gamma,2n)$ cross section obtained from this measurement agrees well with the shape and absolute magnitude of available $(\gamma,2n)$ data.

The (e,α) cross section in ^{65}Cu is in disagreement with previous measurements in magnitude and shape. The (γ,α) cross section derived from our measurements has the expected resonant shape and fits well in the systematics of nuclei in this mass re-

gion. The $E1$ and $E2$ components of the (γ,α) cross section are both small but the $E2$ component is relatively more important.

ACKNOWLEDGMENTS

The authors would like to thank Prof. Giorgio Moscati and Prof. J. Goldemberg for many useful discussions and for reading the manuscript, and Conselho Nacional de Desenvolvimento Científico e Tecnológico, Fundação de Amparo à Pesquisa do Estado de São Paulo, and Financiadora de Estudos e Projectos for financial support.

-
- ¹E. Woly nec, W. R. Dodge, R. G. Leicht, and E. Hayward, Phys. Rev. C 22, 1012 (1980).
²W. R. Dodge, R. G. Leicht, E. Hayward, and E. Woly nec, Phys. Rev. C 24, 1952 (1981).
³W. W. Gargaro and D. S. Onley, Phys. Rev. C 4, 1032 (1971).
⁴C. W. Soto Vargas, D. S. Onley, and L. E. Wright, Nucl. Phys. A 288, 45 (1977).
⁵T. Tamae, T. Urano, M. Hirooka, and M. Sugawara, Phys. Rev. C 21, 1758 (1980).
⁶T. Tanaka, Res. Rep. Lab. Nucl. Sci., Tohoku Univ. 14, 137 (1981), and private communication.
⁷H. Ströher, R. D. Fisher, J. Drexler, K. Huber, U. Kneissl, R. Ratzek, H. Ries, W. Wilke, and H. J. Maier, Phys. Rev. Lett. 47, 318 (1981).
⁸L. A. Smith, R. N. H. Haslam, and J. G. V. Taylor, Phys. Rev. 84, 842 (1951).
⁹J. C. Ritter and R. E. Larson, Nucl. Phys. A127, 399 (1969).
¹⁰J. L. Mathews and R. O. Owens, Nucl. Instrum. Methods 111, 157 (1973).
¹¹J. J. Murphy II, H. J. Gehrhardt, and D. M. Skopik, Nucl. Phys. A277, 69 (1977).
¹²J. J. Murphy II, D. M. Skopik, J. Asai, and J. Uegaki, Phys. Rev. C 18, 736 (1978).
¹³S. C. Fultz, R. L. Blamblett, J. F. Caldwell, and R. R. Harvey, Phys. Rev. 133, B1149 (1964).